

# On super-Poissonian behavior of the Rosenzweig-Porter model in the non-ergodic extended regime

Richard Berkovits

*Department of Physics, Jack and Pearl Resnick Institute, Bar-Ilan University, Ramat-Gan 52900, Israel*

The Rosenzweig-Porter model has seen a resurgence in interest as it exhibits a non-ergodic extended phase between the ergodic extended metallic phase and the localized phase. Such a phase is relevant to many physical models from the Sachdev-Ye-Kitaev model in high-energy physics and quantum gravity, to the interacting many-body localization in condensed matter physics and quantum computing. This phase is characterized by fractal behavior of the wavefunctions, and a postulated correlated mini-band structure of the energy spectrum. Here we will seek evidence for the latter in the spectrum. Since this behavior is expected on intermediate energy scales spectral rigidity is a natural way to tease it out. Nevertheless, due to the Thouless energy and ambiguities in the unfolding procedure, the results are inconclusive. On the other hand, by using the singular value decomposition method, clear evidence for a super-Poissonian behavior in this regime emerges, consistent with a picture of correlated mini-bands.

The Anderson metal-insulator transition continues to surprise even after six decades [1]. The canonical picture for a single particle Anderson transition is the three dimensional Anderson model which shows a metal-insulator transition for a critical value of on-site disorder. For weak disorder the system is metallic and the wave function is extended, while for stronger disorder the wave function is localized and the system is insulating [2, 3]. At the critical disorder the wave function is fractal [4]. The energy spectrum also reflects these phases. In the localized regime the level spacing distribution (corresponding to small energy scales, large times) follow the Poisson distribution, while for the extended regime corresponds to the Wigner-Dyson (WD) distribution. [5–8]. Several forms of the level spacing were suggested at criticality [9–12]. For larger energy scales, the spectral rigidity, i.e., the variance of the number of levels in a given energy window is a useful indicator. For the localized phase the variance is equal to the average number of states in this window, while for the extended phase it is proportional to the logarithm of the average. At the critical point the variance is proportional to the average number of states, with a proportionality lower than one [13–15].

An additional energy scale relevant to disordered metals is the Thouless energy  $E_T = g\Delta$  (where  $g$  is the dimensionless conductance, and  $\Delta$  the average level spacing) [13]. While WD predictions hold up to an energy scale  $E < E_T$ , above which a non-universal behavior takes over. The physical origin of the Thouless energy is the onset of diffusive behavior.

There has been a recent surge in interest in the critical behavior of the transition. Part of this interest stems from the realization that for the many body localization phenomenon the localized and extended regions may be separated by a critical regime [16–25]. An additional motivation pertains to the Sachdev-Ye-Kitaev (SYK) model, originally introduced in the study of spin liquids [26] and recently gaining relevance to holographic dualities in string theory [27] and quantum gravity [28]. There

is evidence the SYK model perturbed by a single-body term shows a critical region [29]. This model also shows a signature of the existence of a Thouless energy [30].

The generalized Rosenzweig-Porter random matrix model (GRP) [31, 32] is considered the most simple model for which the localized and fully ergodic phases both exist, with an non-ergodic extended (NEE) phase separating them. Almost all evidence for the NEE comes from the study of the fractality of the wave functions [32–37]. In Ref. 38 some tantalizing clues for a super-Poissonian behavior have appeared in the  $n$ -th level spacing distribution. Finding fingerprints for NEE in the energy spectrum is important, for both theoretical and practical reasons. It is much easier numerically, as well as experimentally, to obtain the energies than wavefunctions for large systems. Here, we examine two methods to garner such information. The venerable method of spectral rigidity (number variance) [39], and singular value decomposition (SVD) [40–42]. Both will be used to study very large GRP matrices on scales of thousands of eigenvalues. It turns out that although the spectral rigidity exhibits anomalies which could be attributed to NEE, it is nevertheless hard to separate them from the effects of the Thouless energy, finite size, and dependence on unfolding. On the other hand, SVD seems to provide strong evidence for an intermediate scale of energy, for which systems belonging to the NEE phase show super-Poissonian behavior of the spectra, similar to the random Cantor set behavior [17].

The GRP is defined by a random matrix  $H_{ij}$ , of size  $N \times N$ , where the diagonal terms are chosen from a certain distribution while the off diagonal term is chosen from a distribution with a variance proportional to  $N^{-\gamma}$ . Specifically, we have chosen the diagonal  $H_{ii}$  from a box distribution with a range  $-\sqrt{6}/2 \dots \sqrt{6}/2$  ( $\delta^2 \langle H_{ii} \rangle = 1/2$ ) and the off-diagonal  $H_{i \neq j}$  from a box distribution between  $-N^{-\gamma/2}/2 \dots N^{-\gamma/2}/2$  ( $\langle \delta^2 H_{i \neq j} \rangle = N^{-\gamma}/12$ ), thus corresponding to  $N^\gamma \langle H_{i \neq j}^2 \rangle / \langle H_{ii}^2 \rangle = 1/6$ .

For GRP one expects a transition from localized to

extended behavior at  $\gamma = 2$  [32, 38, 45–50]. This transition shows in the nearest neighbor level distribution that switches from a Poisson behavior for  $\gamma > 2$  to WD repulsion at  $\gamma < 2$ . In the supplementary material[51] we show the finite size scaling of the ratio statistics, substantiating this transition at  $\gamma = 2$ .

On the other hand, the transition between the NEE phase to the truly extended phase anticipated to occur at  $\gamma = 1$ , leaves no signature in the ratio statistics. This is expected, as small energy scale correspond to long times, and since the states are extended at very long times both in the ergodic as well as the NEE phases, short energy scales can not resolve the difference. Thus, one should probe energy scales that are much larger than the mean level spacing.

Two statistical measures will be considered: level number variance for a given energy window and applying the singular value decomposition (SVD) on the spectrum [40–42].

The first is also known as spectral rigidity [39]. Specifically, for an energy window of a size  $E$ , the average number of levels,  $\langle n(E) \rangle$ , and the variance,  $\langle \delta^2 n(E) \rangle = \langle (n(E) - \langle n(E) \rangle)^2 \rangle$  are calculated. For the WD distribution  $\langle \delta^2 n(E) \rangle = 0.44 + (2/\pi^2) \ln(\langle n(E) \rangle)$ , while for the Poisson distribution  $\langle \delta^2 n(E) \rangle = \langle n(E) \rangle$ . One may argue that for the NEE phase ( $1 < \gamma < 2$ ) one should expect  $\langle \delta^2 n(E) \rangle = \chi \langle n(E) \rangle$ , where  $\chi = \gamma - 1$  [38, 52].

A major concern for the variance method is that it relies on unfolding of the spectrum. For a rather smooth spectra, the details of unfolding and averaging over realizations should not affect the results, but for the NEE phase, where a non-smooth spectral density is expected [17, 30, 38], the unfolding procedure might strongly influence results. A different way to study the properties of an ensemble of spectra originating from different realizations has been recently suggested [40–42], based on techniques originating in signal analysis. Given  $L$  realizations of  $P$  eigenvalues each, one defines a matrix  $X$  of size  $L \times P$  where  $X_{lp}$  is the  $p$  level of the  $l$ -th realization.  $X$  is SVD decomposed as  $X = U \Sigma V^T$ , where  $U$  and  $V$  are  $L \times L$  and  $P \times P$  matrices correspondingly, and  $\Sigma$  is a diagonal matrix of size  $L \times P$  and rank  $r = \min(L, P)$ . The  $r$  diagonal elements of  $\Sigma$ , denoted as  $\sigma_k$  are the singular values of  $X$  and may be ordered such that  $\sigma_1 \geq \sigma_2 \geq \dots \sigma_r$ . Essentially this is a non-periodic mode decomposition of the series. Defining  $\lambda_k = \sigma_k^2$  represents the fraction of the total variance in the series captured by the mode. The lower singular values capture the global trends of the spectra, while the higher values represent the local fluctuations. It has been postulated that for the for higher values in the localized regime  $\lambda_k \sim k^{-2}$  while in the extended regime  $\lambda_k \sim k^{-1}$  [41, 42], corresponding to 1/f noise behavior [43].

We have calculated  $\langle \delta^2 n(E) \rangle$  for large matrices of size  $N = 16000, 24000, 32000, 48000$  and corresponding 800, 200, 100, 100 different realizations. For each realiza-

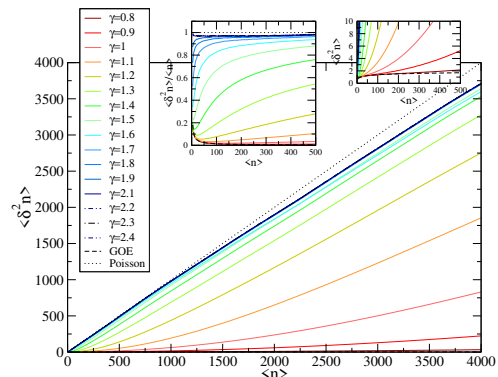


FIG. 1. The variance  $\langle \delta^2 n(E) \rangle$  as function of  $\langle n(E) \rangle$  for the largest matrix size  $N = 48000$  and values of  $\gamma$  between 0.8 to 2.4. The Poisson and Wigner Dyson behavior are indicated. The top right inset zooms into the logarithmic behavior region, where deviations from the Wigner Dyson behavior is seen even deep in the extended ergodic regime  $\gamma < 1$ . The middle inset the variance normalized by  $n$  is plotted. Even in the localized regime  $\gamma > 2$  some deviation from the Poisson value of 1 is seen.

tion  $N$  eigenvalues,  $\epsilon_i$ , were obtained. The spectrum was then unfolded by  $\varepsilon_i = \varepsilon_{i-1} + 2m(\epsilon_i - \epsilon_{i-1}) / \langle \epsilon_{i+m} - \epsilon_{i-m} \rangle$  where  $\langle \dots \rangle$  is an average over realizations, and  $m = 6$  (other values were used with no significant change). The center of the energy window is set at  $E(j) = N/2 + j \cdot 20$ , where for each realization  $j = -j_{max} \dots j_{max}$  (with  $j_{max} = 150, 225, 300, 450$ , i.e. the center of the energy window is located within a range of 3/16 of the spectra around the middle). For each  $E(j)$ , the number of states in a window of width  $E$  centered at  $E(j)$ ,  $n_j(E)$  is evaluated, then the averages  $\langle n(E) \rangle$  and  $\langle n^2(E) \rangle$  are taken over all positions of the center  $j$  and realizations.

The variance  $\langle \delta^2 n(E) \rangle$  as function of  $\langle n(E) \rangle$  is plotted in Fig. 1 for the largest matrix size  $N = 48000$  and different values of  $\gamma$ . Our main aim is to study the asymptotic behavior of the variance at large energy windows. Clearly as  $\gamma$  increases the variance switches from a Wigner-Dyson like behavior to a Poisson like behavior. Nevertheless, the observed behavior raises serious doubts on our ability to give definite answers on the asymptotic behavior from such data. Several factors compound the problem. It is clear that even for  $\gamma < 1$  for which Wigner Dyson behavior ( $\langle \delta^2 n(E) \rangle = (2/\pi^2) \ln(\langle n(E) \rangle) + 0.44$ ) is expected, this behavior is followed only up to a certain  $n_{Th}$ , above which a stronger than linear dependence is seen. This scale  $n_{Th}$  depends both on  $\gamma$  (see right insert in Fig. 1) and on the size of the matrix (see Fig. 2a). This is similar to the deviation seen for the Anderson model [13, 14, 44] and in the SYK model [30], and is an indication for an energy scale, known as the Thouless energy,  $E_{Th} = \delta n_{Th}$  related to a time scale  $t_{Th} = \hbar/E_{Th}$  indicating the typical time necessary to explore the avail-

able system phase space system.  $n_{Th}$  grows as the the system becomes less sparse (lower  $\gamma$ ) or larger in size.

As can be seen in Fig. 1 for  $\gamma > 2$ , and for different sizes in Fig. 2b, deep in the Poisson regime ( $\gamma > 2$ ), the expected Poisson behavior ( $\langle \delta^2 n(E) \rangle = \langle n(E) \rangle$ ) is seen up to some value of  $n$  ( $n \sim 1000$  for  $N = 48000$  and  $n \sim 500$  for  $N = 16000$ ). Above this value  $\langle \delta^2 n(E) \rangle$  grows weaker than linear. One could speculate that these deviations are a result of combination of finite size effects and the unfolding which becomes less reliable at larger scales.

For the intermediate values of  $1 < \gamma < 2$ , where the NEE regime is expected, the behavior is even messier (Fig. 1 and Fig. 2c). Almost immediately the variance starts growing much faster than linear. As  $n$  increases, the growth patters out. One might fit a linear behavior with a smaller than one slope, corresponding to the expected  $\langle \delta^2 n(E) \rangle = \chi \langle n(E) \rangle$  behavior. Nevertheless, larger values  $n$  remain strongly dependent on the size of the matrix (Fig. 2c). Thus, it is difficult to tease out the behavior at large  $n$  without ad-hoc assumptions on the range of the fit.

Due to these difficulties, we switch to the SVD method, which does not require unfolding. The scree plots of the ordered partial variances,  $\lambda_k$ , for 800 realizations of matrix size  $N = 16000$  and  $0.8 < \gamma < 2.4$  is presented in Fig. 3. Large  $k$  corresponds to small energy scales, Large energy scales depend on the overall density of states, which is not universal, and therefore no information can be gleaned from  $k \sim 1$ . For the Poisson regime ( $\gamma \geq 2$ , indicated by purple symbols)  $\lambda_{k>2}$  follows the expected  $k^{-2}$  behavior [41, 42], up to deviations for large values of  $k > 500$ . In the WD regime ( $\gamma \leq 1$ , indicated by reddish symbols), for  $k \geq 10$ ,  $\lambda_k$  follows  $k^\alpha$ , with a slope  $\alpha \sim 0.8$  – different than the expected slope  $\alpha = 1$ . As discussed in the supplementary material [51], this is the effect of a finite number of realizations, much smaller than the number of eigenvalues ( $L \ll P$ ). So for small energy scales, the WD behavior is followed up to an energy scale, which may be identified as  $E_{th}$  (corresponding to a value  $k_{Th}$ ) above which a much steeper decent of  $\lambda_{k < k_{Th}}$  is observed. This is in line with the number variance behavior.

The NEE regime ( $1 < \gamma < 2$ ) shows intermediate behavior between WD behavior at large  $k$  and Poisson at small values of  $k$ . This general behavior is expected, since as can be deduced from Fig. 2c, at very short energy scales WD behavior is expected. At values of  $\gamma > 1.6$  strong deviations from Poisson are seen at large values of  $k$ , and for  $\gamma < 1.6$  large values of  $k$  show clear correspondence with WD. The rang of energies for which WD holds increases as  $\gamma$  decreases. For large energies (small  $k$ ), the complementary behavior is evident, Poisson behavior is followed, where for larger  $\gamma$  the Poisson curve is joined earlier. Thus, for large energies the spectra follows Poisson behavior in agreement with the expectations of Ref. 52.

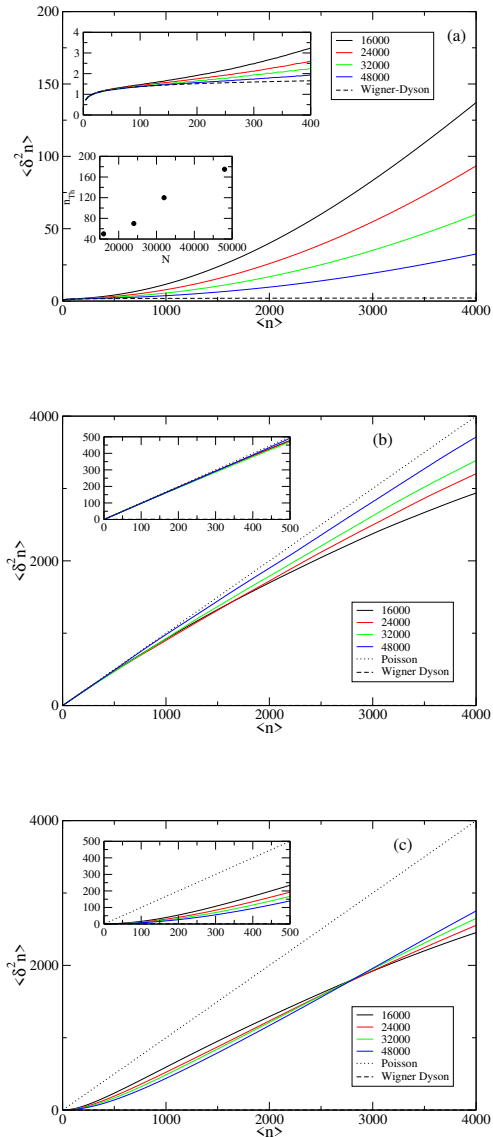


FIG. 2. The variance  $\langle \delta^2 n(E) \rangle$  as function of  $\langle n(E) \rangle$  for (a)  $\gamma = 0.8$  (WD regime); (b)  $\gamma = 2.4$  (Poisson regime); (c)  $\gamma = 1.2$  (NEE regime); and matrix sizes between  $N = 16000$  and  $N = 48000$ . A zoom into smaller values of  $n$  is shown in the inset. (a) Deep in the WD regime, it is clear that at  $n_{Th}$  deviations from the WD behavior are seen. The dependence of  $n_{Th}$  on size is presented in the lower inset in (a). Above  $n_{Th}$  the variance grows stronger than linear and depends on  $N$ . (b) Deep in the Poisson regime. Up to  $n \sim 500$  the behavior is linear as expected from the Poisson regime. For higher  $n$  deviations to weaker dependence is seen. For larger systems the deviation appears for larger values of  $n$ . (c) In the NNE regime, the behavior deviates from WD almost immediately and follows a stronger than linear behavior, up to a point where a weaker dependence on  $n$  is seen.

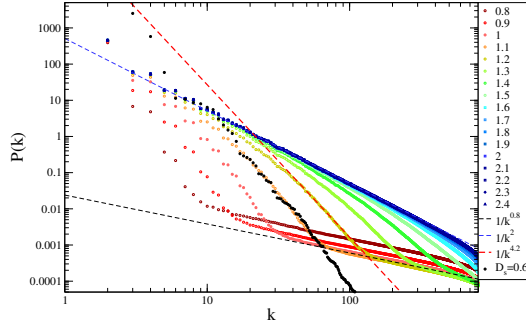


FIG. 3. The the scree plots of ordered partial variances,  $\lambda_k$ , for 800 realizations of matrix size  $N = 16000$  and different values of  $\gamma$  between 0.8 to 2.4. The expected behavior for Poisson ( $1/k^2$ ), WD ( $1/k^{0.8}$ ), and the transient behavior at  $\gamma = 1.2$  ( $1/k^{4.2}$ ) are indicated by dashed lines. A random Cantor set spectra of  $N = 4000$  and 1000 realization with  $D_s = 0.6$  (see text) corresponds to the full black circles.

The crossover between the WD and Poisson behavior at intermediate values of  $k$  is most pronounced for  $1 < \gamma < 1.6$ . It seems that for a significant range of  $k$  a definite slope is followed, with a slope larger than Poisson (super-Poisson), which depends on  $\gamma$ . This is demonstrated for  $\gamma = 1.2$  where a fit to  $1/k^{4.2}$  is drawn. It is evident that a good fit in the range  $40 < k < 120$  is obtained. A super-Poisson (or multi-fractal metal) behavior has its origin in clustering of eigenvalues related to the mini-band structure [17, 38] for which the correlations between levels belonging to the same cluster (mini-band) are much stronger than between the mini-bands. In Ref. 17 a random Cantor set model which mimics the expected behavior of these mini-bands was proposed. Level spacings  $\Delta$  are drawn independently from a power-law distribution  $P(\Delta > \Delta_0) \sim \Delta_0/\Delta^{1+D_s}$  (where,  $\Delta_0$  is a constant, and  $D_s$  is a measure of fractality of the spectrum). As can be seen in Fig. 3, a random Cantor set, drawn from 1000 realizations of 4000 levels each, with  $D_s = 0.6$ , follows quite strikingly the behavior of  $\gamma = 1.1$  for intermediate values of  $k$ . Similarly, decreasing values of  $D_s$  fit increasing values of  $\gamma$ . This lends strong support to the notion of a fractal (mini-band) structure of the spectrum of the NEE phase for intermediate energy scales.

As for the number variance one may wonder how sensitive is the SVD method to finite size effects. In Fig. 4, we examine the dependence of the scree plot slopes on matrix sizes  $N = 8000, 16000, 24000, 480000$  with 1000, 800, 200, 100 realizations for WD ( $\gamma = 0.8$ ), Poisson ( $\gamma = 2$ ) and the NEE ( $\gamma = 1.2$ ) regime. Since the value of  $\lambda_k$  depends on size, for comparison we multiplied the curves by a constant to shift them one on top of the

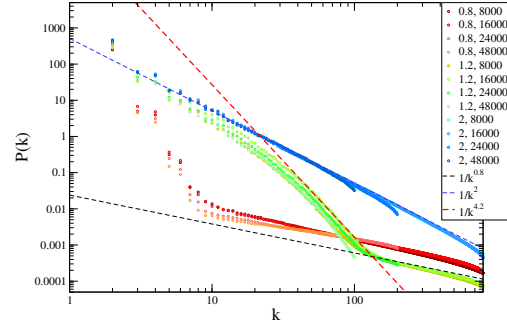


FIG. 4. The the scree plots of ordered partial variances  $\lambda_k$  for different matrix size  $N = 8000, 16000, 24000, 480000$  for 1000, 800, 200, 100 realizations correspondingly, and three different values of  $\gamma = 0.8, 1.2, 2$ . The curves for different matrix sizes were shifted by multiplying them by a constant in order that they will overlap with the curves for  $N = 16000$ . The influence of the number of realizations is depicted by calculating  $\lambda_k$  for  $N = 16000$ , with only 400 and 200 realizations for  $\gamma = 1.2$  (black symbols).

other for the same  $\gamma$ . In all cases a similar behavior of  $\lambda_k$  is seen for all sizes. The same holds for changing the number of realizations. Of course the maximum  $k$  is reduced but the overall behavior remains, as can be seen from Fig. 4 where for  $N = 16000$  and  $\gamma = 1.2$ , with 800, 400 and 200 realizations.

Thus, singular value decomposition reveals robust super-Poissonian behavior for intermediate energy scales of the NEE phase for the parameter range  $1.6 < \gamma < 2$ . For  $1 < \gamma < 1.6$ , it is hard to observe the super-Poissonian regime since it is pushed to smaller energy scales, i.e., larger  $k$ . Moreover, the absolute slope decreases, and thus the deviation from WD is less pronounced. Studying this regime will require a much larger number of realization than is available for this study. Demonstration of super-Poissonian behavior of the SVD analysis of energy spectra of other systems which are expected to show NEE behavior, for example, disordered Josephson junctions array [17] and granular SYK matter [53] may turn out very illuminating.

- 
- [1] P.W. Anderson, Phys. Rev., **109**, 1492 (1958).
  - [2] P. A. Lee and T. V. Ramakrishnan, Rev. Mod. Phys. **57**, 287 (1985).
  - [3] B. Kramer A. MacKinnon, Rep. Prog. Phys. **56**, 1469 (1993).
  - [4] H. Aoki, J. Phys. C **16**, L205 (1983).
  - [5] B. Shklovskii, B. Shapiro, B. R. Sears, P. Lambrianides and H. B. Shore, Phys. Rev. B. **47**, 11487 (1993).
  - [6] T. Guhr, A. Muller-Groeling, H. A. Weidenmuller, Phys.

- Rep. **299**, 190 (1998).
- [7] A.D. Mirlin, Phys. Rep. **326**, 259 (2000).
- [8] R. Evers and A.D. Mirlin, Rev. Mod. Phys. **80**, 1355 (2008).
- [9] V. E. Kravtsov, I. V. Lerner, B. L. Altshuler and A. G. Aronov, Phys. Rev. Lett. **72**, 888 (1994).
- [10] S. N. Evangelou, Phys. Rev. B **49**, 16805 (1994).
- [11] A. G. Aronov, V. E. Kravtsov, and I. V. Lerner, Pis'ma Zh. Eksp. Teor. Fiz. **59**, 40 (1994) [JETP Lett. **59**, 39 (1994)].
- [12] I. Kh. Zharekeshv and B. Kramer, Phys. Rev. Lett. **79**, 717 (1997).
- [13] B. Altshuler and B. Shklovskii, Sov. Phys. JETP [Zh. Eksp. Teor. Fiz. 91,220] **64**, 127 (1986).
- [14] B. Altshuler, I. Zarekeshv, S. Kotochigova, and B. Shklovskii, Sov. Phys. JETP [Zh. Eksp. Teor. Fiz. 94, 343] **67**, 625 (1988).
- [15] A. G. Aronov and A. D. Mirlin Phys. Rev. B **51**, 6131(R) (1995).
- [16] M. Pino, L. B. Ioffe and B. L. Altshuler, PNAS **113**, 536 (2016).
- [17] M. Pino, V. Kravtsov, B. Altshuler and L. Ioffe, Phys. Rev. B **96**, 214205 (2017).
- [18] T. Mithun, Y. Kati, C. Danieli and S. Flach, Phys. Rev. Lett. **120**, 184101 (2018).
- [19] M. Thudiyangal, C. Danieli, Y. Kati and S. Flach, Phys. Rev. Lett. **122**, 054102 (2019).
- [20] E. J. Torres-Herrera and L. F. Santos, Annalen der Physik **529**, 1600284 (2017).
- [21] R. Berkovits, Annalen der Physik **529**, 1700042 (2017).
- [22] J. Lindinger, A. Buchleitner and A. Rodríguez Phys. Rev. Lett. **122**, 106603 (2019). t
- [23] S. Roy, I. Khaymovich, A. Das and R. Moessner, SciPost Physics **4** 025 (2018).
- [24] L. Faoro, M. Feigelman and L. Ioffe, arXiv:1812.06016 (2018).
- [25] K. Kechedzhi, V. Smelyanskiy, J. R. McClean, V. S. Denchev, M. Mohseni, S. Isakov, S. Boixo, B. Altshuler and H. Neven arXiv:1807.04792 (2018).
- [26] S. Sachdev and J. Ye, Phys. Rev. Lett. **70**, 3339 (1993).
- [27] J. Maldacena, International journal of theoretical physics **38**, 1113 (1999).
- [28] J. Maldacena, S. H. Shenker, and D. Stanford, J. High Energ. Phys. **08** 106 (2016).
- [29] T. Micklitz, F. Monteiro and A. Altland, Phys. Rev. Lett. **123**, 125701 (2019).
- [30] A. M. García-García and J. J. M. Verbaarschot Phys. Rev. D **94**, 126010 (2016)
- [31] N. Rosenzweig and C. E. Porter, Phys. Rev. B **120**, 1698 (1960).
- [32] V. E. Kravtsov, I. M. Khaymovich, E. Cuevas, and M. Amini, New J. Phys. **17** (2015).
- [33] C. Monthus, J. Phys. A: Math. Theor. **50**, 295101 (2017).
- [34] V. Kravtsov, B. Altshuler and L. Ioffe, Ann. Phys. **389**, 148 (2018).
- [35] E. Bogomolny and M. Sieber, Phys. Rev. E **98**, 032139 (2018).
- [36] P. Nosov, I. M. Khaymovich and V. E. Kravtsov, Phys. Rev. B **99**, 104203 (2019).
- [37] M. Pino, J. Tabanera and P. Serna, arXiv:1904.02716.
- [38] G. de Tomasi, M. Amini, S. Bera, I. M. Khaymovich, and V. E. Kravtsov, SciPost Phys. **6**, 14 (2019).
- [39] M. L. Mehta, *Random matrices* (Acad. Press, New York, 1991), 2nd ed.
- [40] R. Fossion, G. Torres-Vargas and J. C. López-Vieyra, Phys. Rev. E, **88**, 060902(R) (2013).
- [41] G. Torres-Vargas, R. Fossion, C. Tapia-Ignacio and J. C. López-Vieyra, Phys. Rev. E, **96**, 012110 (2017).
- [42] G. Torres-Vargas, J. A. Méndez-Bermudez, J. C. López-Vieyra and R. Fossion, Phys. Rev. E, **98**, 022110 (2018).
- [43] A. Relaño, J. M. G. Gómez, R. A. Molina, J. Retamosa, and E. Faleiro, Phys. Rev. Lett. **89**, 244102 (2002).
- [44] D. Braum and G. Montambaux, Phys. Rev. B **52**, 13903 (1995).
- [45] A. Pandey, Chaos Solitons Fractals **5**, 1275 (1995).
- [46] E. Brezin and S. Hikami, Nucl. Phys. B **479**, 697 (1996).
- [47] T. Guhr, Ann. Phys. **250**, 145 (1996).
- [48] A. Altland, M. Janssen, and B. Shapiro, Phys. Rev. E **56**, 1471 (1997).
- [49] H. Kunz and B. Shapiro, Phys. Rev. E **58**, 400 (1998).
- [50] D. Facoetti, P. Vivo, and G. Biroli, Europhys. Lett. **115**, 47003 (2016).
- [51] See Supplemental Material at [URL] for nearest level spacing transition at  $\gamma = 2$  and SVD scree plots of lageg  $1/f$  noise series.
- [52] V. E. Kravtsov, K. A. Muttalib, Phys. Rev. Lett. **79**, 1913 (1997).
- [53] A. Altland, D. Bagrets, and A. Kamenev, Phys. Rev. Lett. **123**, 106601 (2019).

# Supplemental material for “On super-Poissonian behavior of the Rosenzweig-Porter model in the non-ergodic extended regime”

Richard Berkovits

Department of Physics, Jack and Pearl Resnick Institute, Bar-Ilan University, Ramat-Gan 52900, Israel

## INTRODUCTION

In this supplemental material the transition from the extended (NEE) to the localized regime as manifested in the finite size scaling of the nearest level spacing is studied in the first section, while in the next section the SVD scree plot for a large simulated  $1/f$  noise series is discussed.

### NEAREST LEVEL SPACING TRANSITION AT $\gamma = 2$

For generalized Rosenzweig-Porter (GRP) one expects a transition from localized to extended behavior at  $\gamma = 2$  [1–8]. This transition is manifested in the energy spectrum of the system in a transition in the nearest neighbor level distribution between Poisson behavior for  $\gamma > 2$  to Wigner-Dyson like repulsion at  $\gamma < 2$ . The finite size scaling of this behavior is clearly seen by the ratio statistics, defined as:

$$r_s = \langle \min(r_n, r_n^{-1}) \rangle, \quad (1)$$

$$r_n = \frac{E_n - E_{n-1}}{E_{n+1} - E_n},$$

where  $E_n$  is the  $n$ -th eigenvalue of the matrix and  $\langle \dots \rangle$  is an average over different matrices and a range of eigenvalues. For the Poisson distribution one expects  $r_s = 2 \ln(2) - 1 \sim 0.3863$ , while for the WD distribution  $r_s \sim 0.5307$  [9]. Finite size scaling assumes that for  $\gamma > 2$  the value of  $r_s$  approaches the Poisson value as the matrix size grows, while for  $\gamma < 2$ ,  $r$  approaches the WD value. At the transition ( $\gamma = 2$ )  $r$  should be independent of the matrix size. Thus, as one plot  $r_s(\gamma)$  for larger values of  $N$  the curve becomes more step-like and all the curves are expected to cross at the same point. This has been seen in Ref. [10] and is reproduced here for larger matrix sizes. In Fig. 1a we plot  $r(\gamma)$  for  $N = 500, 1000, 2000, 4000, 16000, 48000$  with 12800, 6400, 3200, 1600, 800, 100 different matrices. The curves can be scaled using  $\tilde{\gamma} = |\gamma - \gamma_c|(N/N_0)^\beta$ , with  $\beta = 0.12$ ,  $\gamma_c = 2$  and  $N_0 = 500$  was chosen as the smallest matrix size. As can be seen in Fig. 1b this scaling works well.

Thus, for the low energy scale one finds very clear evidence for the transition between localized states and extended ones at  $\gamma=2$ .

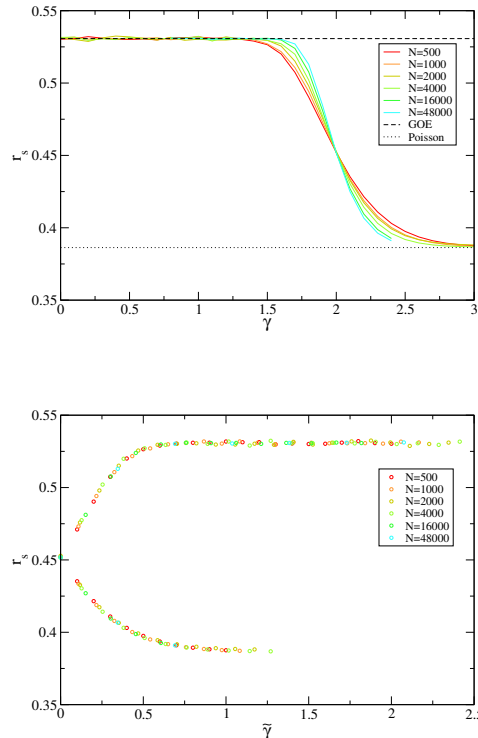


FIG. 1. The nearest neighbor level spacing statistics as manifested in the behavior of the ratio statistics  $r(\gamma)$  for different values of  $\gamma$  and matrix size  $N$ . (a) The finite size dependence of  $r_s(\gamma)$ . All curves cross at the critical value  $\gamma_c = 2$  and exchange their order as they cross this point. This is a clear manifestation of a second order phase transition. (b) Finite size scaling. All curves neatly fall on the two branches above and below the transition as function of  $\tilde{\gamma}$  defined in the text.

### SVD SCREE PLOT OF LARGE $1/f$ NOISE SERIES

By definition a  $1/f$  noise series is a sequence with a power spectrum of  $1/f$ . Such a series may be numerically generated by different methods. Here we apply the method of Kasdin [11], using a recursive filter. We generate  $L = 1600$  realizations with  $P = 8192$  values each ( $\{X_{p=1, P}^{l=1, L}\}$ ), and perform a discrete fast Fourier transform,  $f^l(k) = (1/\sqrt{P}) \sum_p X_p^l \exp(-2\pi i k p/P)$ , and then average the power spectrum over all realizations,

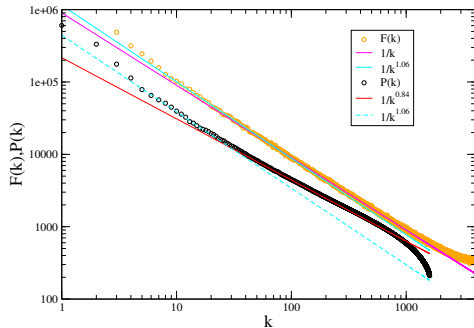


FIG. 2. Power spectrum ( $F(k)$ , orange circles) and Scree plot of the SVD ( $P(k)$ , black circles) of an ensemble of numerically generated  $1/f$  noise sequences of length 8192 for 1600 different realizations. Attempts to fit to different slopes are shown.

$F(k) = \sum_l |f^l(k)|^2/L$  which is shown in Fig. 2. The SVD of the matrix  $X$  is extract as described in the main text and the the scree plot  $P(k)$ , can also be seen in Fig. 2.

The power spectrum shows the expected  $1/k$  for the range  $50 < k < 2000$ . For  $k < 50$ ,  $F(k)$  takes a somewhat larger slope,  $1/k^{1.06}$ . The SVD Scree plot is expected to follow the power spectrum slope [12–14]. Indeed, for  $k < 50$ ,  $P(k)$  follows with the same slope,  $1/k^{1.06}$ , while for,  $50 < k < 1000$   $P(k)$  corresponds to a different slope  $\sim 1/k^{0.84}$ . It is important to note that while for the Fourier transform results in  $0 < k < P/2$  amplitudes and the number of realizations  $L$  determines only the quality

of averaging, for the SVD one is limited to  $L$  eigenvalues. Therefore, if  $P \ll L$ , SVD will show finite number of realization effects for a smaller value of  $k$ , resulting in the fact that although the Fourier transform shows a  $1/k$  slope, the SVD results show a gentler slope. This trend is seen also in the main text, where although one expects the SVD in the Wigner-Dyson regime to show a  $1/k$  slope, it shows a slope closer to  $\sim 1/k^{0.8}$ .

- 
- [1] V. E. Kravtsov, I. M. Khaymovich, E. Cuevas, and M. Amini, *New J. Phys.* **17** (2015).
  - [2] G. de Tomasi, M. Amini, S. Bera, I. M. Khaymovich, and V. E. Kravtsov, *SciPost Phys.* **6**, 14 (2019).
  - [3] A. Pandey, *Chaos Solitons Fractals* **5**, 1275 (1995).
  - [4] E. Brezin and S. Hikami, *Nucl. Phys. B* **479**, 697 (1996).
  - [5] T. Guhr, *Ann. Phys.* **250**, 145 (1996).
  - [6] A. Altland, M. Janssen, and B. Shapiro, *Phys. Rev. E* **56**, 1471 (1997).
  - [7] H. Kunz and B. Shapiro, *Phys. Rev. E* **58**, 400 (1998).
  - [8] D. Facchetti, P. Vivo, and G. Biroli, *Europhys. Lett.* **115**, 47003 (2016).
  - [9] Y. Y. Atas, E. Bogomolny, O. Giraud, and G. Roux, *Phys. Rev. Lett.* **110**, 084101 (2013).
  - [10] M. Pino, J. Tabanera and P. Serna, arXiv:1904.02716.
  - [11] N. J. Kasdin, *Proc. of the IEEE* **83**, 802 (1995).
  - [12] R. Fossion, G. Torres-Vargas and J. C. López-Vieyra, *Phys. Rev. E*, **88**, 060902(R) (2013).
  - [13] G. Torres-Vargas, R. Fossion, C. Tapia-Ignacio and J. C. López-Vieyra, *Phys. Rev. E*, **96**, 012110 (2017).
  - [14] G. Torres-Vargas, J. A. Méndez-Bermudez, J. C. LópezVieyra and R. Fossion, *Phys. Rev. E*, **98**, 022110 (2018).
  - [15] A. Relaño, J. M. G. Gómez, R. A. Molina, J. Retamosa, and E. Faleiro, *Phys. Rev. Lett.* **89**, 244102 (2002).